Journal of Data Acquisition and Processing
ISSN: 1004-9037
https://sjcjycl.cn/
DOI: 10.5281/zenodo.7766293

A MATHEMATICAL MODEL OF FLOW OF BLOOD IN A SEGMENT OF AN ARTERY BY A NON-HOMOGENOUS APPROACH

Subrata Rakshi
Department of Mathematics, Rabindranath Tagore University, Bhopal, India,
rakshit.subrata1983@gmail.com

Bhawna Agrawal
Department of Mathematics, Rabindranath Tagore University, Bhopal, India,
bhawnakhushiagrawal@gmail.com

Sanjeet Kumar
Department of Mathematics Lakshmi Narain College of Technology & Science, Bhopal, India, sanjeetkumarmath@gmail.com

Abstract— In our attempt to simulate blood flow through arteries mathematical modelling for cardiovascular system are popular. These mathematical models are also used to predict the dynamical patterns in the pathological and psychological condition. Due to complexities arising out of mechanical properties of the arterial wall, time dependence and the underlying geometry, any comprehensive model is difficult to find. At some level, simplification attempts have been made up to various degrees, in accordance with the scale of the phenomena under our study. Agrawal, B., Kumar, S., Rakshit, S. (2022). shows a mathematical study of the flow of the non-Newtonian fluid, blood through arterial segment affected by stenosis [20].

The physical dimension of the model is one of our concern. Like electrical circuits, different complex regions of the vascular system are collected in simple compartments and connected to form a closed loop. The desired degree of detail has a correlation with the number of blocks. Many zero-dimensional models (also known as lumped parameter model) have been developed for the cardiovascular system in general or for its specific parts. Usage of such an approach preferred at the developing a model for the circulatory system becomes a possibility. Although, they do not provide any information on the mechanical fluid-wall interaction, but they provide the evolution of the mean flow variables.

One dimensional models are in used, when we deal with the wave Propagation phenomena. Over the cross section, the flow motion equations are arranged, thus obtaining the one dimensional models. A high degree of approximation is included keeping in mind the hypothesis that one spatial dimension is prevalent over the others. In our study we have dealt with a simple one-dimensional model for fluid structure problem describing the flow of blood and the wave propagation in a segment of an artery. The arterial wall is thought of as an axisymmetric membrane that can be deform either in radial or longitudinal direction under the action of the force exerted by the fluid.

Khan, R. A., & Agrawal, B. D. (2021) present explanatory solutions for transient flow of Newtonian fluid through miniature channels with Navier slip limit. The induction of the arrangements depends on Fourier arrangement development in space [16]. In (2021) IA Tantry,

S Wani, B Agrawal shows the effect of radiation on steady MHD boundary layer flow over an exponentially stretching sheet was investigated [17].

Keywords—Digital optimization, artificial intelligence, internet connectivity, cybersecurity, governance, internet of things.

I. INTRODUCTION

1. Wall and fluid interaction

The blood flowing in a compatible vessel is a complex dynamic system and is a real problem with the fluid structure. Fluid movement and wall deformation are mutually affected and their coupling is responsible for effects that cannot be explained by each alone. When interested in the phenomenon of wave propagation, simplified models of the "arterial blood wall" system can be devised. In particular, due to the small deformations of the vascular wall and the unidirectional nature of the blood flow, a one-dimensional model was adopted. Khoja, I. M., & Agrawal, B. (2021) Show that the blood pressure is influenced by both of the cross-sectional area and the length of the blood vessel [21].

1.1 The flow equations

Let us consider a homogeneous fluid in terms of density and viscosity , flowing in a straight, axial, distributable tube of circular cross-section.

The intersecting quasi-1D momentum equation is

$$\frac{\delta v}{\delta t} + v\frac{\delta v}{\delta x} = -\frac{1}{d}\frac{\delta p}{\delta x} + f \qquad (1)$$

Where x is the axial ordinate, is the axial velocity, the transient pressure, both averaged over the cross section, and t denotes time. The viscous term is approximated by the friction term of a constant Poiseuille flow in a tube of radius .

$$f \simeq -\frac{8\eta v}{dR^2} \qquad (2)$$

As a consequence, the wall shear stress is given by

$$\tau = \frac{dv}{dr}\Big|_R \simeq -\frac{4\eta v}{dR} \qquad (3)$$

Strictly speaking, expressions (2) and (3) carry a constant flow in a solid tube, but are considered acceptable for quasi-stationary flows and for small deformations.

The principle of conservation of mass in a deformable tube is expressed by the following continuity equation

$$\frac{\delta R}{\delta t} + \frac{R}{2}\frac{\delta v}{\delta x} + v\frac{\delta R}{\delta x} = 0 \qquad (4)$$

1.2 The Wall equation

The vessel wall is modeled as a symmetrically elastic membrane, which is a thin two-dimensional envelope with negligible mass (wall thickness 0) compared to the fluid in it. The membrane, which does not have bending stiffness, is able to deform under the forces exerted by the fluid (that is, shear stress - cfr. (3) - and transient stress p). Suppose are the Lagrangian coordinates of a particle P with a parametric coordinate along the membrane in its plane of symmetry. In such a frame of reference, the major deformation ratios are in the meridional and circumferential directions, respectively

$$\varepsilon_1 = \sqrt{\left(\frac{dr_p}{ds}\right)^2 + \left(\frac{dx_p}{ds}\right)^2}\,, \varepsilon_2 = \frac{r_p}{R^{\bullet}} \tag{5}$$

Where is the unreformed radius (corresponding to the zero transmural pressure).

Since the fluid equations are expressed in Euler coordinates, let us perform a coordinate transformation and let us indicated by R and S the Eulerian counterparts of the Lagrangian coordinates for a particle of the membrane. In this coordinate system, the extensions (5) are written as

$$\varepsilon_1 = \sqrt{\frac{1+R'^2}{S'^2}} \quad , \quad \varepsilon_2 = \frac{R}{R^*} \tag{6}$$

(the prime denoting x-derivative). The membrane equilibrium equations in tangential and normal directions are provided

$$R'\left(T_1 - T_2\right) + RT_1' = d\tau R\sqrt{\left(1+R'^2\right)},$$

$$\frac{-R^n}{\left(1+R'^2\right)\sqrt{\left(1+R'^2\right)}}T_1 + \frac{1}{R\sqrt{(1+R'^2)}}T_2 = p \tag{7}$$

Let us now introduce a constitutive equation for the arterial vessel which gives an expression for T1 and T2 in equations (7). For an incompressible hyper elastic material, it is possible to define the strain-energy function as a function of the main strains: it represents the elastic energy stored per unit volume in terms of strain and stress variables.

A constitutive stress-energy density function modeling of the mechanical properties of the arterial wall was proposed by Zhou and Fung as.

$$u = c_0\left(e^Q - 1\right), \qquad Q = c_1E_1'^2 + c_2E_2'^2 + 2c_3E_1E_2, \tag{8}$$

where c_0 is a material parameter having the dimensions of dyne/cm, c_1, c_2 & c_3 are non-dimensional constants (with $c_1 \approx c_2$ and $c_1, c_2 \gg c_3$) and $E_k = \frac{1}{2}\left(\varepsilon_k^2 - 1\right), k = 1,2$ are the

principal Green strain. Once the form of u is specified, the mechanical properties are completely determined, being the stress components (averaged across the thickness) along the longitudinal and circumferential directions given by differentiation of u.

$$T_1(\varepsilon_1,\varepsilon_2)=\frac{\varepsilon_1}{\varepsilon_2}\frac{\partial u}{\partial E_1}=\frac{1}{\varepsilon_2}\frac{\partial u}{\partial \varepsilon_1}=2\frac{\varepsilon_1}{\varepsilon_2}c_0e^{Q}\left(c_1E_1+c_3E_2\right), \tag{9}$$

$$T_1(\varepsilon_1,\varepsilon_2)=\frac{\varepsilon_2}{\varepsilon_1}\frac{\partial u}{\partial E_2}=\frac{1}{\varepsilon_1}\frac{\partial u}{\partial \varepsilon_2}=2\frac{\varepsilon_2}{\varepsilon_1}c_0e^{Q}\left(c_3E_1+c_2E_2\right), \tag{10}.$$

The former relations hold in the case of an anisotropic membrane, wherein principal directions of strain and stress coincide and express the property that the instantaneous young's modulus increases with the strain, but with a different amount in the two directions.

2. Boundary conditions and lumped parameter models

The full nonlinear system fluid-structure is modelled by the coupled equations (1), (4), (7) (with the replacements (6), (9), (10)) and a numerical method will be used. The analysis of the linearized problem in the neighborhood of a stressed configuration will be the object of a forthcoming work. The above differential equations have to be solved in a finite domain representing an arterial segment. Such a segment is extracted from the arterial tree and boundary conditions of physical significance for the variables are required. To this aim, the presence of the remaining vascular bed has to be considered. In a pulsatile pressure is assigned at the inlet as a forcing, and a simple Windkessel 3-element parameter model for the termination is proposed. However, when balance of flows and pressures for the systemic circulation have to be taken into account, models for the closed-loop system should be addressed. They are built by partitioning the whole vascular tree in elementary districts and by "lumping" the dynamical variables in each of them (lumped parameter models).
These models date back to the pioneeristic works of

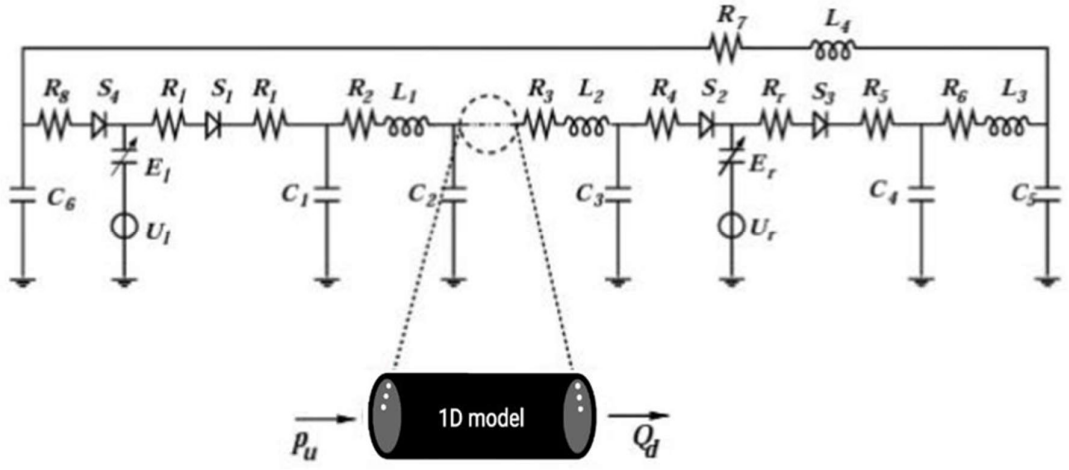

Picture 1: The electrical community analogue to a lumped parameter mannequin at six cubicles for the human circulatory machine (see Avanzolini et al. [1]) and its coupling with the 1D

mannequin at the degree of the descending aorta. Pressure and float variables are exchanged at the interface factors to warranty continuity.

It is also observed by Agrawal, B., Kumar, S., Das, G. (2022), that wall shear stress increases as height of stenosis and porous parameter increase whereas it decreases with the increasing values of velocity of blood and slope of stenosed artery [18]. Damno, M. M., Agrawal, B., Kumar, S., Das, G., (2021). Shows the effects of modeling blood flow through a stenosis and an aneurysm using five different blood rheological models is presented in this investigation. The flow field and wall shear stress distributions produced by each model are investigated for various flow rates and degrees of abnormality. The results show that there are significant differences between simulating blood as a Newtonian or non- Newtonian fluid [19]. Mir, A. M., & Agrawal, B. D. (2021). Concluded that we can utilize our knowledge of gene regulatory apparatus encoded in DNA to produce new microorganisms with unexpected properties [22].

Westerhof et al. and are primarily based on the analogy between hydraulic networks and electrical circuits. In the community proposed by means of Avanzolini et al. [1] for the circulatory system, six sections can be diagnosed (fig. 1). In every compartment the values of the resistance, compliance and in entrance are regular and a linear relationship between waft and stress is given. These basic blocks are linked between them and linked with the coronary heart pump to shape a closed loop representing the cardiovascular system. By putting conservation of strain and of glide in all nodes of the network, a differential linear system.

By setting conservation of pressure and of flow in all nodes of the network, a differential linear system

$$\frac{dX}{dt} = A(\mathrm{t}) + f\left(t, X\right)$$

describing the time evolution of the mean values of the variables X = (pi; Qi) in each compartment is obtained [1]. To account for a comprehensive system of the global circulation, the lumped model (a) and the distributed model (b) presented in the section 2 are coupled. This approach allows to implicitly assign boundary conditions for the system (b). Actually these are easily expressed as a functions of variables of (a) to guarantee the continuity of flow and pressure at the interfaces. Following [3], we have inserted the model (a) in the point of network corresponding to the descending aorta (fig. 1). The coupled system is equivalent to a 1D model for the full circulatory system where, except for a segment, the remaining arterial tree has been truncated and lumped in a finite number of blocks. On the other way around, the coupled model can be regarded as a lumped parameter model where a compartment has been expanded in a distributed model. The connected subsystems (a) + (b) form a unique closed-loop and no boundary condition for the flow variables is required.

If the coupling strategy eliminates the drawback of assigning a boundary value for and , wall displacement conditions at the extrema of the compliant vessel have to be provided. These are given by considering a long (i.e. of length much larger than the reference radius) vessel with free ends.

Therefore, the condition

$$R' = R'' = 0, \qquad S' = 1 \qquad (12)$$

hold at the ends. Such conditions imply (null axial strain - see (6)). From (7.2) it follows that the implicit relation for R

$$R_P = T_2 \qquad (13)$$

(law of Laplace) is prescribed at the boundaries. Moreover, the boundary conditions on S

$$S(0,\mathrm{t}) = 0, \qquad S\left(L,t\right) = L^* \qquad (14)$$

expressing a finite axial deformation are imposed.

Thus, we solve the differential system (11) and the partial differential system (1), (4), (7), together with interface continuity conditions. Details of the coupling algorithm can be found in [5].

3. Numerical results and discussion

To handle the 1D fluid-structure model numerically, the equations (1),(4),(7) are solved simultaneously in a finite interval . Let us consider a sequence of n + 1 equispaced grid points (xi) i =0,……n with and .The spatial discretization is obtained by evaluating membrane strains and stresses (see eqns. (6), (9), (10)) at an inner points of a staggered grid by considering averaged neighboring variables. On the other

hand, wall–fluid equilibrium equations (7) and flow equations (1)- (4) are computed at the n-1 inner points .

In the following numerical experiments, the spatial mesh has been obtained by dividing the length of the vessel L = 8 cm in 800 equal parts (Δx=0.01 cm) and with a time step Δt = s. The 1D model is inserted in correspondence of the descending aortic artery (fig. 1) and is solved coupled with the 0D model. The Runge-Kutta scheme of second order has been used in both the distributed and the lumped parameter model to advance in time. The choice of the above numerical parameters guarantees stability and grid independence. The resulting nonlinear system is solved by a globally convergent Newton type method.

The following numerical values for the distributed model are used:

$$c_1 = 0.38 \qquad c_2 = 0.26 \qquad c_3 = 0.046$$

$$R^* = 0.8cm \qquad L^* = L = 8cm \qquad d = 1.05g/cm^3$$

In large vessels, as that considered here, the frictional force due to the fluid viscosity is comparatively small and wall be neglected ( ).The value of is

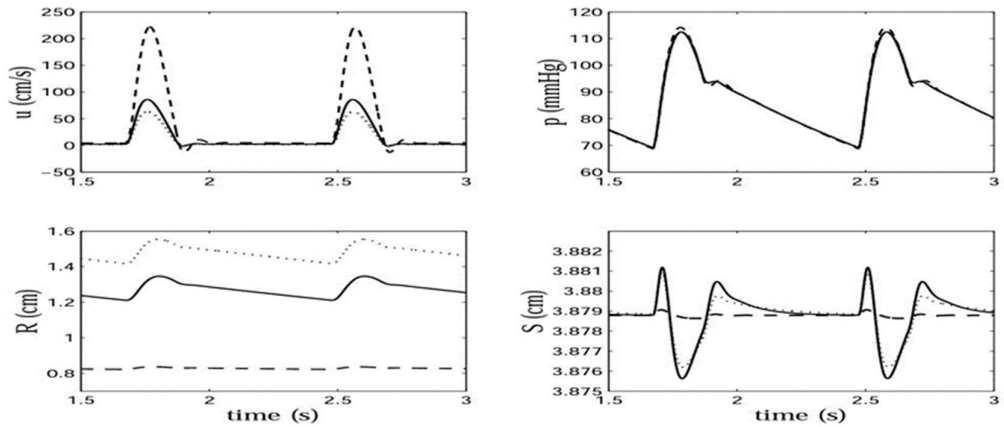

Picture 2: Time histories for u, p, R, S at the center of the artery for three values of the elasticity coefficient

c_0 ($c_0 = 10^5\, dyne/cm$ dotted line . $c_0 = 2.10^5\, dyne/cm$

continuous line , $c_0 = 5.10^6\, dyne/cm$ dashed line.

Varied in the range $c_0 = 10^5 - 10^7\, dyne/cm$ (note that c_0 in (8) is obtained by integration across the wall thickness of the analogous density energy function in Zhou and Fung). For a lower value of c_0 the vessel wall undergoes large deformation that cannot be adequately represented by the present model .For $c_0 \gg 10^7$ the solution approaches to that relative of a rigid tube (see below). Actually, the values of R^*, p and c_0 cannot be chosen independently, but should satisfy a compatibility condition, being c_0 approximately equal to pR (mean values), in the linear case. The lumped parameters have been taken from [1].

Subject to a nice coronary heart pressure, transmitted thru the 0D model, the wall expands and oscillates periodically between a most and a minimal limit. Similarly, all the waft variables have a periodical behavior. Actually we understand imply price and small superposed fluctuations over it. Such values rely on the elasticity coefficient and on the unreformed radius $R*$ .In picture-2 the behavior of the four variables u; p; R; S in the mid-point are depicted for three different values of the parameter c_0 . A small phase lead of p on u is present (see also fig. 4). For larger c_0 the wall becomes stiffer: as expected, both the radial and longitudinal deformations decrease with c_0, being the latter comparatively smaller. Despite no full-size version in the stress is current (a upward shove of the systolic top of the stress is got solely at giant c_0), a sharp make bigger of the waft speed is reported, correspondent to the decreased arterial lumen. Some more oscillations after the systolic height might also be present.

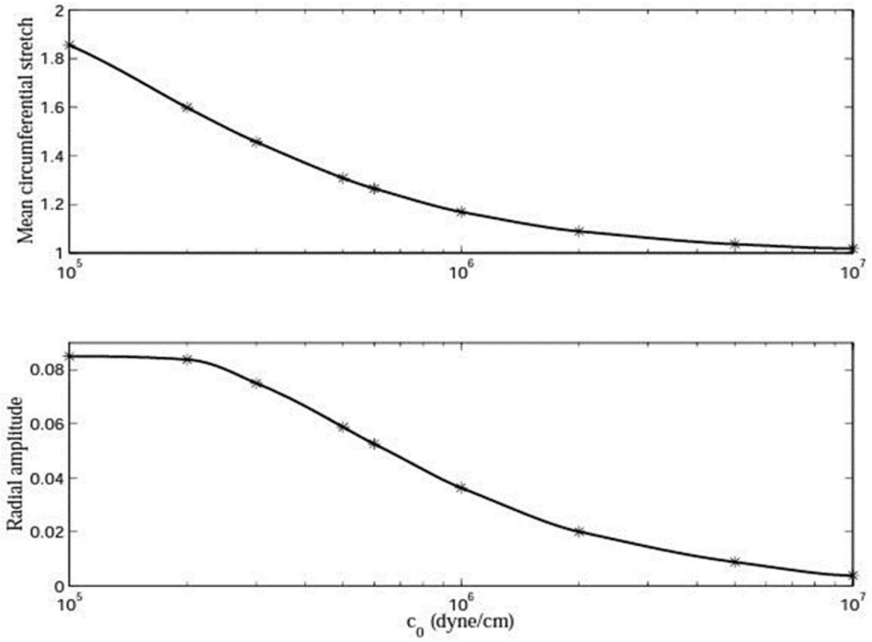

Picture 3: Mean circumferential stretch $\hat{\varepsilon}_2$ (above) and non-dimensional radial amplitude (bottom) $\hat{A}$ (bottom) at the center of the vessel as a function of c_0. Starred

points are results from simulations continuous curves are obtained by a cubic interpolation. Note the different order of magnitude.

To measure the influence of c_0 on the radial deformation, let us introduce the mean deformation - referred to the central point ($x = 4$) and computed over the last two periods – as

$$\hat{R} = \frac{R_{\max} + R_{\min}}{2}$$

The mean circumferential stretch $\hat{\varepsilon}_2 = \frac{\hat{R}}{R*}$ and the non-dimensional radial amplitude $\hat{A} = \frac{R_{\max} - \hat{R}}{R*}$ Both $\hat{\varepsilon}_2$ and $\hat{A}$ drop (the former of 45%, the latter of 95%) with, c_0 in the range considered, until an asymptotic value (picture.3).

The haste of the surge can be attained by fixing two points in the vessel and measuring the crossing time of a peak. still, such a procedure isn't accurate over a short length and for the time and space way as those considered in this work. also the biographies change their shape as they travel, and it's delicate follow a profile time. As a consequence, the computed speed value measured for v, p and R between the same grid points may be different, and varies in time. For $c_0 = 2.10^5 dyne/cm$ an averaged value of the speed for v wave is found of about
6-7 m/s.

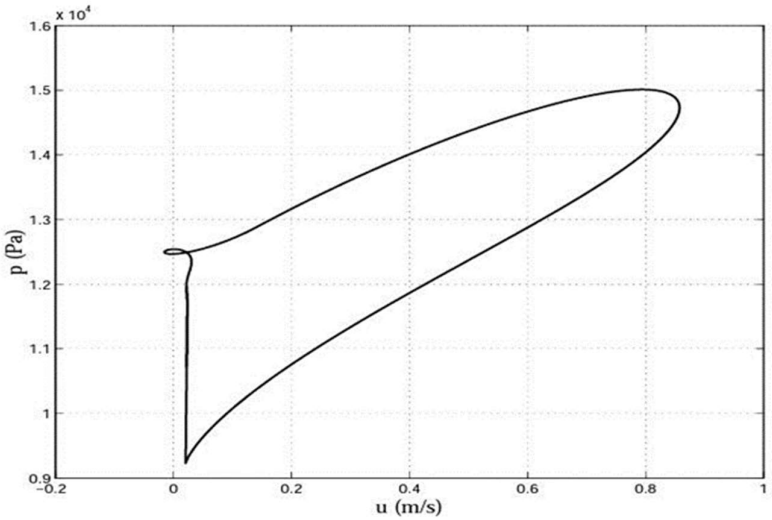

Picture4: PU loop curve for in the central point of the vessel. Slopes of such a curve indicates the local wave speed. A phase lag between the two variables is present.

Khir and Parkers suggest another method to measure the wave speed in elastic tubes in absence of reflected waves. It is based on the validity of the water hammer equation and consists in measuring the slope of the PU loop curves. For a typical PU loop as that displayed in picture-4, the local wave speed is in agreement with experiments.

4. Conclusions

The dynamics of the flow of blood in the segment of an artery has been studied in relation to the elastic and nonlinear properties of the vessel wall. One dimensional model used to describe the mechanical fluid wall interaction. The one-dimensional model was expressed by a set of

four non-linear partial differential equations. The effects of the elastic parameter son the flow and on the wall deformations are shown by numerical experiments.
In spite of the limitations, the model offers a predictive insight in propagation phenomena and can be easily generalized to account for vessel tampering and bending.

References

1. Avanzolini, G., Barbini, P., Cappello, A., & Cevenini, G. (1988). CADCS simulation of the closed-loop cardiovascular system. International journal of bio-medical computing, 22(1), 39-49.
2. Pedrizzetti, G. (1998). Fluid flow in a tube with an elastic membrane insertion. Journal of Fluid Mechanics, 375, 39-64
3. Formaggia, L., Nobile, F., Quarteroni, A., & Veneziani, A. (1999). Multiscale modelling of the circulatory system: a preliminary analysis. Computing and visualization in science, 2(2), 75-83.
4. Almeder, C. R. (1999). Hydrodynamic modelling and simulation of the human arterial blood flow (Doctoral dissertation).
5. Di Carlo, A., Nardinocchi, P., Pontrelli, G., & Teresi, L. (2002). The role of the arterial prestress on blood-flow dynamics.
6. Khir, A. W., & Parker, K. H. (2002). Measurements of wave speed and reflected waves in elastic tubes and bifurcations. Journal of biomechanics, 35(6), 775-783.
7. Di Carlo, A., Nardinocchi, P., Pontrelli, G., & Teresi, L. (2003). A heterogeneous approach for modelling blood flow in an arterial segment. Simulation in Biomedicine V (eds. ZM Arnez, CA Brebbia, F. Solina & V. Stankovski), WIT Press, 69-78.
8. Pontrelli, G. (2006). The role of the arterial prestress in blood flow dynamics. Medical engineering & physics, 28(1), 6-12.
9. Amadori, D., Ferrari, S., & Formaggia, L. (2007). Derivation and analysis of a fluid-dynamical model in thin and long elastic vessels. Networks & Heterogeneous Media, 2(1), 99
10. Bárdossy, G., & Halász, G. (2011). Modeling blood flow in the arterial system. Periodica Polytechnica Mechanical Engineering, 55(1), 49-55.
11. Kitawaki, T. (2012). Numerical simulation model with viscoelasticity of arterial wall. In Viscoelasticity-From Theory to Biological Applications (pp. 55-61). IntechOpen.
12. Wang, X., Delestre, O., Fullana, J. M., Saito, M., Ikenaga, Y., Matsukawa, M., & Lagrée, P. Y. (2012). Comparing different numerical methods for solving arterial 1d flows in networks. Computer Methods in Biomechanics and Biomedical Engineering, 15(1), 61-62.
13. Dobroserdova, T. K., Vassilevski, Y. V., Simakov, S. S., Olshanskii, M. A., Salamatova, V. Y., Gamilov, T. M., & Ivanov, Y. A. (2015). The model of global blood circulation and applications. In 6th European Conference of the International Federation for Medical and Biological Engineering (pp. 403-406). Springer, Cham.
14. Berntsson, F., Karlsson, M., Kozlov, V., & Nazarov, S. A. (2016). A one-dimensional model of viscous blood flow in an elastic vessel. Applied Mathematics and Computation, 274, 125-132.

15. Canuto, D., Chong, K., Bowles, C., Dutson, E. P., Eldredge, J. D., & Benharash, P. (2018). A regulated multiscale closed-loop cardiovascular model, with applications to hemorrhage and hypertension. International Journal for Numerical Methods in Biomedical Engineering, 34(6), e2975.
16. Khan, R. A., & Agrawal, B. D. (2021). Analysis of fluid flow through channels with slip Boundary: Mathematical study. International Journal of Statistics and Applied Mathematics, 6(1), pp134-137 https://www.mathsjournal.com/pdf/2021/vol6issue1/PartB/6-1-7-685.pdf
17. IA Tantry, S Wani, B Agrawal - Int J Stat Appl Math, 2021. Study of MHD boundary layer flow of a Casson fluid due to an exponentially stretching sheet with radiation effect. 6(1), pp 138-144 https://www.mathsjournal.com/pdf/2021/vol6issue1/PartB/6-1-9-857.pdf
18. Agrawal, B., Kumar, S., Das, G. (2022). Mathematical model of blood flow through stenosed arteries with the impact of hematocrit on wall shear stress. International Journal of Applied Research, 8(3), pp 439-443. https://www.researchgate.net/publication/361634077_Impact_Factor_84_IJAR_2022 https://www.allresearchjournal.com/archives/2022/vol8issue3/PartF/8-3-90-606.pdf
19. Damno, M. M., Agrawal, B., Kumar, S., Das, G., (2021). A mathematical model for the blood flow in a modeled artery with a stenosis and an aneurysm. International Journal of Statistics and Applied Mathematics, 6(2), pp 65-71. https://www.mathsjournal.com/pdf/2021/vol6issue2/PartA/6-3-4-512.pdf
20. Agrawal, B., Kumar, S., Rakshit, S. (2022). A mathematical study of constrained fluid movement in the arterial system due to the formation of multiple stenosis. International Journal of Applied Research, 8(3), pp 455-464. https://www.allresearchjournal.com/archives/2022/vol8issue3/PartF/8-3-101-230.pdf
21. Khoja, I. M., & Agrawal, B. (2021). Mathematical modeling of blood flow. International Journal of Statistics and Applied Mathematics, 6(4), pp116-122. https://www.mathsjournal.com/pdf/2021/vol6issue4/PartB/6-4-24-502.pdf
22. Mir, A. M., & Agrawal, B. D. (2021). A mathematical study of DNA complexes of one-bond edge type. Journal of Mathematical problems equations and Statistics, 2(2), pp 08-16. https://www.mathematicaljournal.com/article/12/1-1-20-526.pdf